Characterization of Different Stent Designs through Numerical Modelling

Earl Go-Aco* and Homer Co
[1] Manufacturing Engineering and Management Department
De La Salle University
*Corresponding Author: earl_go-aco@dlsu.edu.ph

Abstract: Diseases of the heart is the leading cause of mortality in the Philippines. Coronary artery disease is the most common which, at early stages, can be treated through angioplasty surgery and stenting. The coronary stents have a probability of failing due to restenosis and is linked to their different characteristics. In addition, there are hundreds of different stent designs available in the market today with each having its own combination of design and material. Finite-element analysis (FEA) is a widely used technique in gathering data by carrying out simulations especially in the field of biomedical engineering where phenomena happening inside the body can be conveniently simulated. The objective of the study is to characterize stents with different geometries and materials with the use of FEA. The process involved creating CAD models of the systems in contact namely the stent, balloon, artery, and blood using a CAD software and simulating their interaction with one another through finite-element analysis. A total of three stent designs were used taking into consideration their varying mesh geometry and material namely stainless steel, cobalt chromium and platinum chromium. Stent deployment in angioplasty was recreated using the software which involves inflating the balloon which expands the stent and deflating the balloon thereafter. Afterwards, blood was introduced and a computational fluid dynamics simulation was carried out. The stents yielded different stresses effected on the arterial walls which, in high values, increases the possibility of restenosis. Stainless steel yielded the highest stress on the artery followed by cobalt chromium while platinum chromium had the least. Blood flow profile was different as well for each stent design depending on the mesh geometry.

Key Words: stent; finite element analysis; computational fluid dynamics

1. INTRODUCTION

1.1 Subsection

According to the Department of Health in the Philippines (2006), diseases of the heart is ranked first in the leading causes of mortality in the country with a rate of 95.5% in every 100,000 of the population. The most common disease of the heart is the Coronary Artery Disease. A coronary heart disease is an ailment that happens when fatty material and other substances form plaque and build-up along the arterial walls thus blocking the blood flow (Michaels et al., 2002). Such disease happens due to tobacco smoking, unhealthy diet, and lack of physical activity which all add up to an unhealthy lifestyle (Banzon, 2013). At present, there are two ways on how to treat coronary heart disease through surgery. One way is through coronary artery bypass surgery which involves rerouting the pathway for the blood to flow by using a healthy artery somewhere else in the body. Another way is through Angioplasty Surgery wherein a small-wire-mesh tube, called coronary stent, is inserted through the artery which provides scaffolding to support a damaged arterial wall.

In previous years, extensive research has been made on coronary stents resulting in numerous design and material use. These stents behave differently from one another as they are subjected to a variety of contact forces upon deployment in the artery which are taken into account in the making of the stent. The main problem that stents are faced with is restenosis, which is defined as the recurrence of a blockage in the artery after treatment. Restenosis rate is related with arterial wall stress and can be changed by adjusting stent design (Lally et al., 2005). Blood flow also contributes as it exerts force along its direction of flow. The stent should be able to withstand such forces subjected to it and not cause vascular injury along the arterial walls in contact with it. Thus, there is an interplay between stent design, material, and coating.

2. METHODOLOGY

Similar to other studies, the simulation of stent deployment and blood flow is made to be as realistic as possible. The conceptual approach of the study is shown in Fig. 1.
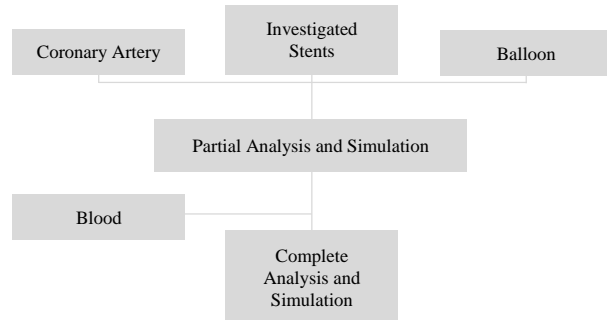

Fig. 1. Conceptual Framework

Finite Element Analyzing software allow the creation of steps with different boundary conditions and loading parameters in order to carry out efficient simulations. With the presence of a fluid, the human blood, it is essential to have a concept built on a two-step process. The first step consists of the interaction between the artery, the balloon, and the chosen investigated stents while the second step is set up solely for fluid analysis and simulation.

2.1 Modelling
2.1.1 Geometry Creation

A 3D computer model of each stent as well as the artery, plaque and blood will be made using a CAD software. The study makes use of three stent models: Kaname, Promus, and Firebird whose geometries are to be modelled as reported in open sources and are named in this study as Stent A, Stent B, and Stent C respectively. The criteria involved in the selection of the stent models are material and geometry diversity. Each of the stent will represent the three widely used materials in stent manufacturing: Cobalt-Chromium,

Platinum-Chromium, and Stainless Steel. Also, the stent selection was restricted to stents made available to the Philippine market as approved by the Food and Drugs Administration. Table 1 shows the geometrical properties of the investigated stents:

Table 1. Stent Geometry Properties

Stent	A	B	C
Outer Diameter	1.65 mm	1.65 mm	1.67 mm
Strut Width	0.09 mm	0.08 mm	0.1 mm
Strut Thickness	0.08 mm	0.08 mm	0.1 mm
Length	8 mm	8 mm	8 mm
Material	CoCr L605	PtCr	316L Stainless Steel
Geometry Reference	Kaname	Promus Element	Firebird

A cylindrical hollow tube will represent the artery as an idealized vessel with an inner diameter of 2.7 mm and an outer diameter of 4.5 mm. This cylinder is then split into three concentric layers representing the three layers of the artery: the intima, media, and adventitia having the thickness of 0.24 mm, 0.32 mm, and 0.34 mm respectively. The plaque will be modelled as calcified plaque having an internal diameter of 2.1 mm and a length of 6 mm centered along the artery wall. A solid cylindrical tube will then represent the blood with its outer surface contoured to the inner surface of the stent, artery and plaque.

2.1.2 Mesh Generation

In order to determine the ideal mesh sizes for the finite element analysis, a mesh convergence study will be done on each CAD model. Each model will first be subjected to arbitrary loading and boundary conditions. Mesh sizes will then be changed on this set-up until the corresponding output converges to a

certain value or reaches an established tolerance value.

2.1.3 Material Properties

The material properties of each stent material (i.e. elastic modulus, Poisson's ratio, mass density) will be based on external references as the stent manufacturers do not disclose such data readily to the public. As for the artery, plaque and blood, the material properties will also be referenced other researches and references. The stents and their corresponding materials are as follows:

Table 2. Stent Material Properties

Material	CoCr L605	PtCr	316L Stainless Steel
Density	9100 kg/m^3	9900 kg/m^3	8000 kg/m^3
Young's Modulus	243 GPa	203 GPa	193 GPa
Poisson's Ratio	0.29	0.29	0.3
Elongation %	50	45	60
Tensile Strength	1000 MPa	834 MPa	595 MPa
0.2% Yield Strength	500 MPa	480 MPa	275 MPa

The arterial wall will be modelled as a hyperelastic material following the Mooney-Rivlin model equation using the test data in the study of the mechanical properties of human coronary arteries by Holzapfel et. al. (2005). Each of the three layers of the artery will have their own material properties based on these test data (see Appendix B). A polyurethane material will be assigned to the balloon following an isotropic hyperelastic model with the following parameters:

Table 3. Balloon Material Properties

Parameters	C10	C01	D1	Poisson's Ratio	Density
Poly-urethane	1.03 176	3.692 66	0	0.495	1070 kg/m^3

The plaque will be taken as a hyperelastic material following the Ogden model equation having the material properties of a calcified plaque.

Table 4. Plaque Material Properties

Parameters	μ_i	α_i	D_i
Calcified Plaque	93000	8.17	4.3e^{-7}

Blood will be modelled as an incompressible viscous fluid governed by Navier-Stokes equations with values taken from the study done by Dehlaghi et al (2007) as follows:

Table 5. Blood Material Properties

Parameters	Density	Dynamic Viscosity
Blood	0.056 kg/m^3	0.00345 Pa·s

2.1.4 Boundary Conditions

A total of four contact pairs is established namely: balloon and stent, stent and plaque, stent and artery, and blood and artery. A surface-to-surface hard contact will be set between all contact pairs to represent the normal behavior while a penalty with a Columb frictional coefficient of 0.1 is set for the tangential behavior along the interior arterial wall as well as along the surface of the plaque. The stent is then to be imposed on the balloon with a frictionless surface contact and all three models, artery, stent and balloon, are to be coaxially constrained. For the fluid-structure interaction simulation, an interaction surface will be set on the interior arterial wall, the plaque surface, and on the exposed parts of the stent as blood flows through the system. The corresponding interaction surface pair will be the outer surface of the modelled blood. Zero pressure value will be set at the inlet and a velocity profile will be set at the outlet using the data used by Martin et al (2014) in simulating the pulsatile flow behavior during a cardiac cycle represented by a varying profile with a peak value of 0.43 m/s.
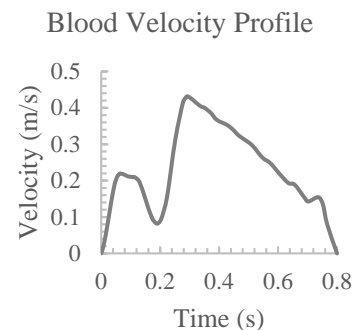

Fig. 2. Blood Velocity Profile (taken from Martin et al, 2014)

2.2 Simulation

Blood will be modelled as an incompressible viscous fluid The simulation is divided into two steps: stent deployment and blood interaction which will be done on each stent model.

2.2.1 Stent Deployment

The first set-up will contain the artery, stent, and balloon. A uniform constant pressure is applied along the inner surface of the balloon to simulate its inflation. When the stent has been fully deployed, the aforementioned applied pressure is then deactivated, a built in feature of the software, and a negative pressure is then applied in place of it to simulate the deflation of the balloon and to allow the recoil of both the artery and the stent. The output deformed mesh geometry of the artery and the stent are then exported and saved to different files which are to be used in the other half of the simulation.

2.2.2 Blood Interaction

The second set-up will be between the artery, stent, and blood. The resulting geometries of the previous step will be imported onto the set-up. The CAD model of the blood is to be made here as a cylinder whose outer surface is following the deformed geometry of the resulting inner surface made by the merging of the stent and the artery. The simulation that will be done is a Fluid Structure Interaction which is a widely used method involving a deformable or movable structure interacting with an internal or surrounding fluid flow.

The study will make use of the in-house coded algorithms provided by the finite element software together with the governing equations that will be solved on the mesh.

3. RESULTS AND DISCUSSION

Reaching the full deployment diameter marks the end of the simulation and the visualization techniques and features of the software are used to show the resulting deformed geometries of each model. Sufficient pressure was applied on the balloon such that the percentage blockage of the plaque is reduced to < 0.1%. Having different designs, each stent model needed different deployment pressures to reach full deployment. 1.2 MPa was used as deployment pressure for Stent A, 1.5 MPa for Stent B, and 1.3 MPa for Stent C. A time increment of 1e^{-5} was set for the simulation step. Fig. 3 illustrates the how the Mises stresses are distributed on the stent models as well as the location where the peak stress value is experienced. As can be observed, the results show that high stress values are concentrated on the curved, U-shaped, joints. This high concentration is particularly located at the point where the curved geometry comes in tangent with the stems being joint together.
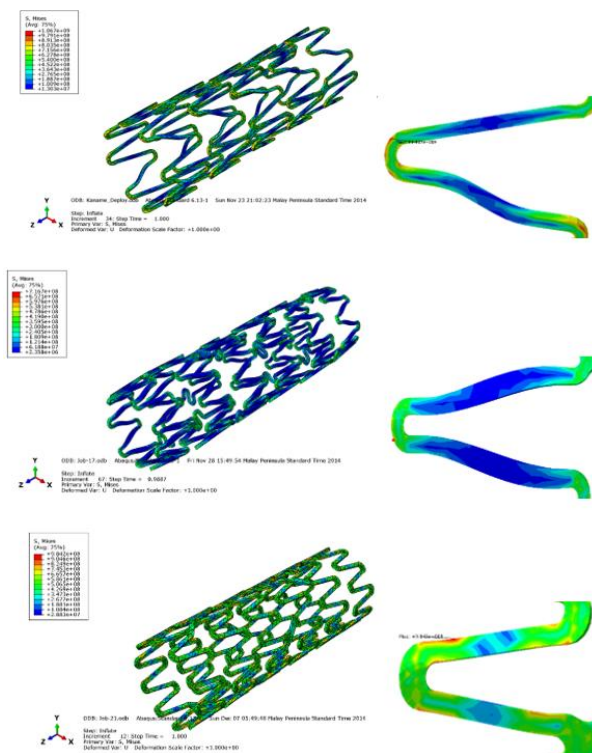

Fig. 3. Stent Contour Plots (from top: Stent A, B, C)

Fig. 4 shows the behavior of the stress values experienced per change in displacement. The behavior of the graph is akin to each material's behavioral properties. Stent C has relatively smaller stress levels experienced with a maximum value of approximately 540 MPa compared to stent A and B having approximate maximum stress values at 1067 and 984 MPa respectively. This is due to the fact that Stainless Steel has a lower yield stress than CoCr or PtCr. The percentage difference between the stress values of stent A and B resulted in 7.78% and stent B and C yielded 45% difference.
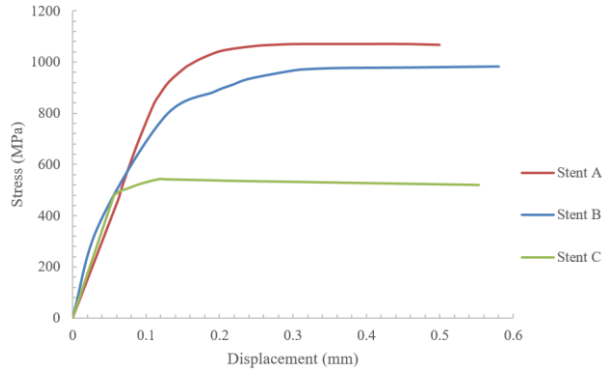
Fig. 4. Displacement vs Stress Graph

Fig. 5 shows a graph of the relationship between the radial displacement of the stent and the equivalent stress experienced by the artery. Artery A experiences a maximum von Mises stress of 0.182 MPa which is located at the point where a curved edge of the U-shaped strut is in contact with the plaque. Artery B, meanwhile, has a maximum von Mises stress of 0.136 MPa located at an area in between two U-shaped struts. Artery C resulted with a maximum von Mises stress of 0.306 MPa which is located also at an area in between opposing struts.
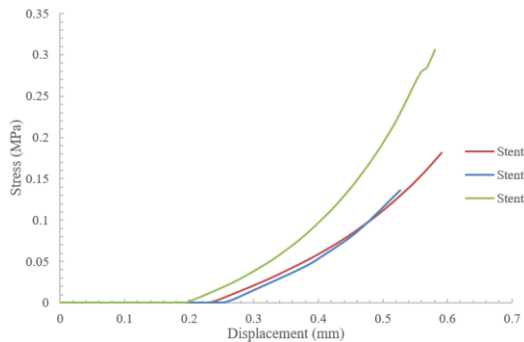

Fig. 5. Stent Displacement vs Artery Stress

From the results of the blood interaction, it was observed that the maximum stress was experienced at the peak of the velocity profile of 0.43 m/s after approximately 0.28 seconds. These stresses were located at surfaces normal to the direction of the velocities. Stent A has a maximum von Mises stress value of $1.034e^{-3}$ MPa, stent B has a value of $9.885e^{-4}$ MPa, and stent C meanwhile has $1.745e^{-4}$ MPa. Consequently, stent A had the lowest total surface area normal to the velocity vector at 12.64 mm². Stent B comes second with a total surface area of 15.38 mm² and stent C had the highest with 18.61 mm². Getting the percentage differences of the stress values, stents A and B had a 4.4% difference and stents B and C resulted in an 82% difference.
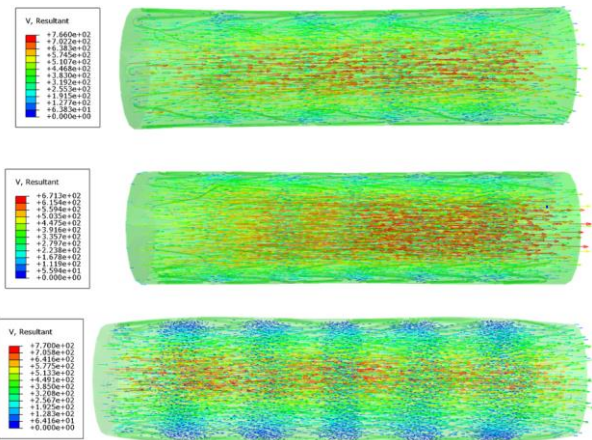

Fig. 6 Blood flow velocity profile (from top: A, B and C)

In summary, the results show that Stent C, made of Stainless Steel, has the lowest yield stress and has the least von Mises stress value but affected the arterial wall the most. Having high stresses on the arterial wall increases the risk of vascular injury which results in an increased probability of restenosis. Stent A, made of CoCr, has the highest yield stress and von Mises stress value at full deployment but had the least effect on the arterial wall. Stent B, made of PtCr, has yield stress and von Mises stress values in between A and C but has the lowest effect on the arterial wall before reaching 4.8 mm radial displacement. The maximum von Mises stress experienced by the stents was commonly found concentrated on the U-shaped

joints. Upon the introduction of blood, Stent A has the highest stress value followed by B and then by C. The stresses were concentrated at the surfaces normal to blood flow and low blood velocities are gathered at the spaces in between the stent struts. The resulting stresses brought by the flow of blood had the same behavior as the resulting stresses from stent deployment with the use of the percentage differences presented earlier. Stent C has a noticeable difference as compared with A and B.

4. CONCLUSIONS

The characterization of different stent designs in this study affirmed that it is a vital factor in the reduction of the rate of failure of coronary stents. The yield stress value of a stent is proportional to the von Mises stress that it experiences upon deployment and is inversely proportional to the stress that the artery is affected with. Subsequently, high artery stresses increase the chance of vascular injury resulting in restenosis. Thus, one way of decreasing this restenosis-inducing stress is by reducing rigidity and increasing conformity of the stent. The stents made from L605 Cobalt-Chromium and Platinum-Chromium have roughly similar stress values experienced as well as effected due to the small difference in material properties.

Blood flow has different magnitudes of effect on the stent depending on the stent design. The variation of the stresses between different stent designs caused by blood flow follows a similar variation during stent deployment. Also, the longer the distance of the struts are from one another, the higher the clump of low velocity profiles are between them. Numerical modelling and simulation is an effective way of conducting tests in a system especially ones that are otherwise difficult or costly to carry out. The study successfully recreated a part

of the process of angioplasty surgery which is the deployment of the stent as well as conducted a characterization of different stent designs.

Although the aim of the study was to bring the simulations close to the actual system, possible room for improvements were seen in the creation of the models. The accuracy of the results can be increased by making use of a micro-computed tomography (Micro-CT) scans in creating the models. This allows the creation of more detailed geometrical models especially the artery and plaque which are irregularly shaped. A broader range of stent designs can be included to capture more stent categories. This includes biodegradable stents as well as self-apposing stents, just to name a few. In this study, blood was modelled as having a constant dynamic viscosity. A more accurate blood model can be made by setting fluid viscosity as a function of shear strain.

5 . ACKNOWLEDGMENTS

6. REFERENCES

A. Schiavone, L.G. Zhao, A.A. Abdel-Wahab, Effects of material, coating, design and plaque composition on stent deployment inside a stenotic artery—Finite element simulation, Materials Science and Engineering: C, Volume 42, 1 September 2014, Pages 479-488, ISSN 0928-4931, 10.1016/j.msec.2014.05.057.

Ahmet Erdemir, Trent M. Guess, Jason Halloran, Srinivas C. Tadepalli, Tina M. Morrison, Considerations for reporting finite element analysis studies in biomechanics, Journal of Biomechanics, Volume 45, Issue 4, 23 February 2012, Pages 625-633, ISSN 0021-9290, 10.1016/j.jbiomech.2011.11.038.

Allison C Morton, David Crossman, Julian Gunn, The influence of physical stent parameters upon restenosis, Pathologie Biologie, Volume 52, Issue 4, May 2004, Pages 196-205, ISSN 0369-8114, 10.1016/j.patbio.2004.03.013.

Angioplasty and Stent Placement. (2012, August 24). In MedlinePlus. Retrieved from http://www.nlm.nih.gov/medlineplus/ency/article/007473.htm

Banzon, E. P. (2013, February 12). Diseases of the Heart. Business Mirror. Retrieved from http://businessmirror.com.ph/index.php/news/opinion/9165-diseases-of-the-heart?tmpl=component&page=

C. Lally, F. Dolan, P.J. Prendergast, Cardiovascular stent design and vessel stresses: a finite element analysis, Journal of Biomechanics, Volume 38, Issue 8, August 2005, Pages 1574-1581, ISSN 0021-9290, 10.1016/j.jbiomech.2004.07.022.

D.K. Liang, D.Z. Yang, M. Qi, W.Q. Wang, Finite element analysis of the implantation of a balloon-expandable stent in a stenosed artery, International Journal of Cardiology, Volume 104, Issue 3, 10 October 2005, Pages 314-318, ISSN 0167-5273, 10.1016/j.ijcard.2004.12.033.

David M. Martin, Eoin A. Murphy, Fergal J. Boyle, Computational fluid dynamics analysis of balloon-expandable coronary stents: Influence of stent and vessel deformation, Medical Engineering & Physics, Volume 36, Issue 8, August 2014, Pages 1047-1056, ISSN 1350-4533, 10.1016/j.medengphy.2014.05.011.

David Roylance. (2001). Finite Element Analysis. Retrieved from http://ocw.mit.edu/courses/materials-science-and-engineering/3-11-mechanics-of-materials-fall-1999/modules/fea.pdf

George Dangas, MD; Frank Kuepper, MD. Restenosis: Repeat Narrowing of a Coronary Artery. Circulation. 2002; 105: 2586-2587 doi: 10.1161/01.CIR.0000019122.00032.DF

Guidance for Industry and FDA Staff, Non-Clinical Engineering Tests and Recommended Labeling for Intravascular Stents and Associated Delivery Systems. U.S. Department of Health and Human Services, Food and Drug Administration, Center for Devices and Radiological Health, 2010.

Ian Pericevic, Caitríona Lally, Deborah Toner, Daniel John Kelly, The influence of plaque composition on underlying arterial wall stress during stent expansion: The case for lesion-specific stents, Medical Engineering & Physics, Volume 31, Issue 4, May 2009, Pages 428-433, ISSN 1350-4533, 10.1016/j.medengphy.2008.11.005.

J. Tiu, G.H. Yeoh, C. Liu. (2008). Computational Fluid Dynamics: A Practical Approach. Massachusetts, MA: Butterworth-Heinemann.

Lally C, Reid AJ, Prendergast PJ. Elastic behaviour of porcine coronary artery tissue under uniaxial and equibiaxial tension. Ann Biomed Eng 2004; 32:1355–64.

M. Azaouzi, N. Lebaal, A. Makradi, S. Belouettar, Optimization based simulation of self-expanding Nitinol stent, Materials & Design, Available online 26 March 2013, ISSN 0261-3069, 10.1016/j.matdes.2013.03.012.

M. Azaouzi, A. Makradi, S. Belouettar, Numerical investigations of the structural behavior of a balloon expandable stent design using finite element method, Computational Materials Science, Volume 72, May 2013, Pages 54-61, ISSN 0927-0256, 10.1016/j.commatsci.2013.01.031.

M. Azaouzi, J. Petit, A. Makradi, S. Belouettar, O. Polit, On the numerical investigation of cardiovascular balloon-expandable stent using finite element method, Computational Materials Science, Volume 79, November 2013, Pages 326-335, ISSN 0927-0256, 10.1016/j.commatsci.2013.05.043.

Matthieu De Beule, Peter Mortier, Stéphane G. Carlier, Benedict Verhegghe, Rudy Van Impe, Pascal Verdonck, Realistic finite element-based stent design: The impact of balloon folding, Journal of Biomechanics, Volume 41, Issue 2, 2008, Pages 383-389, ISSN 0021-9290, 10.1016/j.jbiomech.2007.08.014.

Maurel W, Wu Y, Magnenat N, Thalmann D. Biomechanical models for soft tissue simulation. Berlin: Springer; 1998.

N. Eshghi, M.H. Hojjati, M. Imani, A.M. Goudarzi, Finite Element Analysis of Mechanical Behaviors of Coronary Stent, Procedia Engineering, Volume 10, 2011, Pages 3056-3061, ISSN 1877-7058, 10.1016/j.proeng.2011.04.506.

Narasaiah, G. Lakshmi, Finite Element Analysis, Global Media, Hyderabad, IND, 2008, Page 27.

Republic of the Philippines Department of Health. (2006). Philippine Health Statistics: Leading Causes of Mortality [Data file]. Retrieved from http://www.doh.gov.ph/node/198.html

S.N. David Chua, B.J. MacDonald, M.S.J. Hashmi, Finite element simulation of slotted tube (stent) with the presence of plaque and artery by balloon expansion, Journal of Materials Processing Technology, Volumes 155–156, 30 November 2004, Pages 1772-1779, ISSN 0924-0136, 10.1016/j.jmatprotec.2004.04.396.

Vahab Dehlaghi, Mohammad Tafazoli Shadpoor, Siamak Najarian, Analysis of wall shear stress in stented coronary artery using 3D computational fluid dynamics modeling, Journal of Materials Processing Technology, Volume 197, Issues 1–3, 1 February 2008, Pages 174-181, ISSN 0924-0136, 10.1016/j.jmatprotec.2007.06.010.

W.H. Leung, M.L. Stadius, E.L. Alderman, Determinants of normal coronary artery dimensions in humans, Circulation. 1991; 84:2294-2306 doi: 10.1161/01.CIR.84.6.2294

Wei Wu, Wei-Qiang Wang, Da-Zhi Yang, Min Qi, Stent expansion in curved vessel and their interactions: A finite element analysis, Journal of Biomechanics, Volume 40, Issue 11, 2007, Pages 2580-2585, ISSN 0021-9290, 10.1016/j.jbiomech.2006.11.009.

Zhonghua Sun, Lei Xu, Computational fluid dynamics in coronary artery disease, Computerized Medical Imaging and Graphics, Available online 16 September 2014, ISSN 0895-6111, 10.1016/j.compmedimag.2014.09.002.